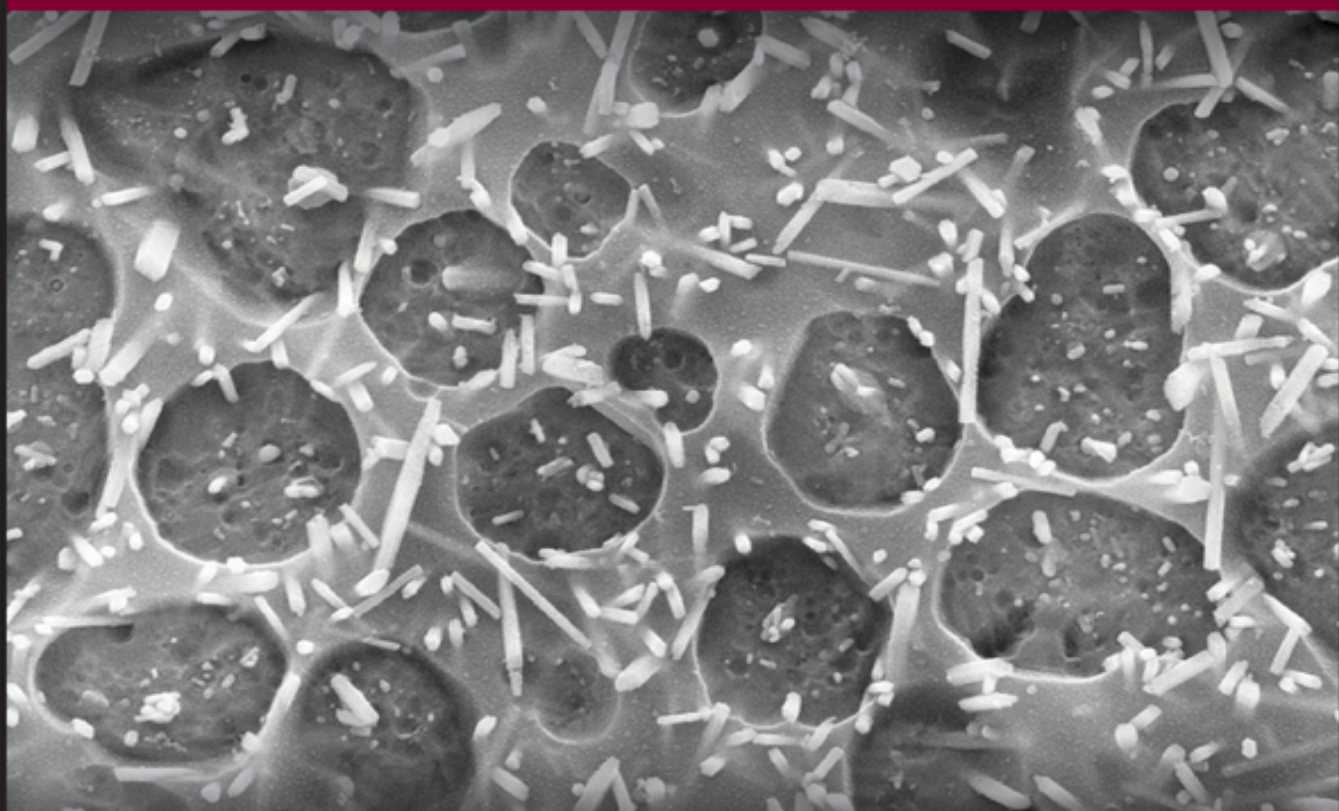


WOLFRAM HÖLAND | GEORGE H. BEALL

GLASS-CERAMIC TECHNOLOGY

THIRD EDITION



Glass-Ceramic Technology

Glass-Ceramic Technology

Third Edition

Wolfram Höland

George H. Beall



WILEY

Copyright © 2020 by The American Ceramic Society. All rights reserved.
Published by John Wiley & Sons, Inc., Hoboken, New Jersey.
Published simultaneously in Canada.

Edition History

John Wiley & Sons Inc. (2e, 2012).
John Wiley & Sons Inc. (1e, 2002)

All rights reserved. No part of this publication may be reproduced, stored in a retrieval system, or transmitted, in any form or by any means, electronic, mechanical, photocopying, recording or otherwise, except as permitted by law. Advice on how to obtain permission to reuse material from this title is available at <http://www.wiley.com/go/permissions>.

The right of Wolfram Höland and George H. Beall to be identified as the authors of this work has been asserted in accordance with law.

Registered Office

John Wiley & Sons, Inc., 111 River Street, Hoboken, NJ 07030, USA

Editorial Office

111 River Street, Hoboken, NJ 07030, USA

For details of our global editorial offices, customer services, and more information about Wiley products visit us at www.wiley.com.

Wiley also publishes its books in a variety of electronic formats and by print-on-demand. Some content that appears in standard print versions of this book may not be available in other formats.

Limit of Liability/Disclaimer of Warranty

In view of ongoing research, equipment modifications, changes in governmental regulations, and the constant flow of information relating to the use of experimental reagents, equipment, and devices, the reader is urged to review and evaluate the information provided in the package insert or instructions for each chemical, piece of equipment, reagent, or device for, among other things, any changes in the instructions or indication of usage and for added warnings and precautions. While the publisher and authors have used their best efforts in preparing this work, they make no representations or warranties with respect to the accuracy or completeness of the contents of this work and specifically disclaim all warranties, including without limitation any implied warranties of merchantability or fitness for a particular purpose. No warranty may be created or extended by sales representatives, written sales materials or promotional statements for this work. The fact that an organization, website, or product is referred to in this work as a citation and/or potential source of further information does not mean that the publisher and authors endorse the information or services the organization, website, or product may provide or recommendations it may make. This work is sold with the understanding that the publisher is not engaged in rendering professional services. The advice and strategies contained herein may not be suitable for your situation. You should consult with a specialist where appropriate. Further, readers should be aware that websites listed in this work may have changed or disappeared between when this work was written and when it is read. Neither the publisher nor authors shall be liable for any loss of profit or any other commercial damages, including but not limited to special, incidental, consequential, or other damages.

Library of Congress Cataloging-in-Publication Data

Names: Höland, Wolfram, author. | Beall, G. H., author.

Title: Glass-ceramic technology / Wolfram Höland, George H. Beall.

Description: Third edition. | Hoboken, New Jersey : Wiley-American Ceramic Society, [2020] | Includes bibliographical references and index. |

Identifiers: LCCN 2019015638 (print) | LCCN 2019017325 (ebook) | ISBN 9781119423713 (Adobe PDF) | ISBN 9781119423706 (ePub) | ISBN 9781119423690 (hardcover)

Subjects: LCSH: Glass-ceramics.

Classification: LCC TP862 (ebook) | LCC TP862 .H65 2019 (print) | DDC 620.1/44—dc23

LC record available at <https://lccn.loc.gov/2019015638>

Cover Design: Wiley

Cover Image: Courtesy of Wolfram Höland

Set in 10/12pt WarnockPro by SPi Global, Chennai, India

Printed in United States of America

10 9 8 7 6 5 4 3 2 1

Contents

Introduction to the Third Edition *xi*

History *xiii*

| | | |
|----------|--|----------|
| 1 | Principles of Designing Glass-Ceramic Formation | 1 |
| 1.1 | Advantages of Glass-Ceramic Formation | 1 |
| 1.1.1 | Processing Properties | 1 |
| 1.1.2 | Thermal Properties | 2 |
| 1.1.3 | Optical Properties | 3 |
| 1.1.4 | Chemical Properties | 3 |
| 1.1.5 | Biological Properties | 3 |
| 1.1.6 | Mechanical Properties | 3 |
| 1.1.7 | Electrical and Magnetic Properties | 3 |
| 1.2 | Factors of Design | 4 |
| 1.3 | Crystal Structures and Mineral Properties | 4 |
| 1.3.1 | Crystalline Silicates | 4 |
| 1.3.1.1 | Nesosilicates | 5 |
| 1.3.1.2 | Sorosilicates | 5 |
| 1.3.1.3 | Cyclosilicates | 5 |
| 1.3.1.4 | Inosilicates | 6 |
| 1.3.1.5 | Phyllosilicates | 7 |
| 1.3.1.6 | Tectosilicates | 7 |
| 1.3.2 | Phosphates | 27 |
| 1.3.2.1 | Apatite | 27 |
| 1.3.2.2 | Orthophosphates and Diphosphates | 29 |
| 1.3.2.3 | Metaphosphates | 30 |
| 1.3.3 | Oxides | 31 |
| 1.3.3.1 | TiO ₂ | 32 |
| 1.3.3.2 | ZrO ₂ | 32 |
| 1.3.3.3 | MgAl ₂ O ₄ (Spinel) | 33 |
| 1.4 | Nucleation | 34 |
| 1.4.1 | Homogeneous Nucleation | 36 |
| 1.4.2 | Heterogeneous Nucleation | 38 |
| 1.4.3 | Kinetics of Homogeneous and Heterogeneous Nucleation | 39 |
| 1.4.4 | Limits of the Classical Nucleation and Crystallization Theory (CNT) and New Approaches | 42 |
| 1.4.5 | Examples of Applying the Nucleation Theory in the Development of Glass-Ceramics | 44 |

| | | |
|----------|---|-----------|
| 1.4.5.1 | Internal (Volume) Nucleation | 44 |
| 1.4.5.2 | Surface Nucleation | 48 |
| 1.4.5.3 | Temperature–Time–Transformation Diagrams | 50 |
| 1.5 | Crystal Growth | 53 |
| 1.5.1 | Primary Growth | 54 |
| 1.5.2 | Anisotropic Growth | 55 |
| 1.5.3 | Surface Growth | 61 |
| 1.5.4 | Dendritic and Spherulitic Crystallization | 62 |
| 1.5.4.1 | Phenomenology | 62 |
| 1.5.4.2 | Dendritic and Spherulitic Crystallization Applications | 64 |
| 1.5.5 | Secondary Grain Growth | 64 |
| 2 | Composition Systems for Glass-Ceramics | 67 |
| 2.1 | Alkaline and Alkaline Earth Silicates | 67 |
| 2.1.1 | SiO ₂ –Li ₂ O (Lithium Disilicate) | 67 |
| 2.1.1.1 | Stoichiometric Composition | 67 |
| 2.1.1.2 | Nonstoichiometric Multicomponent Compositions | 69 |
| 2.1.2 | SiO ₂ –BaO (Sanbornite) | 78 |
| 2.1.2.1 | Stoichiometric Barium Disilicate | 78 |
| 2.1.2.2 | Multicomponent Glass-Ceramics | 79 |
| 2.2 | Aluminosilicates | 80 |
| 2.2.1 | SiO ₂ –Al ₂ O ₃ (Mullite) | 80 |
| 2.2.2 | SiO ₂ –Al ₂ O ₃ –Li ₂ O (β-Quartz Solid Solution, β-Spodumene Solid Solution) | 82 |
| 2.2.2.1 | β-Quartz Solid Solution Glass-Ceramics | 82 |
| 2.2.2.2 | β-Spodumene Solid Solution Glass-Ceramics | 86 |
| 2.2.3 | SiO ₂ –Al ₂ O ₂ –Na ₂ O (Nepheline) | 88 |
| 2.2.4 | SiO ₂ –Al ₂ O ₃ –Cs ₂ O (Pollucite) | 91 |
| 2.2.5 | SiO ₂ –Al ₂ O ₃ –MgO (Cordierite, Enstatite, Forsterite) | 93 |
| 2.2.5.1 | Cordierite Glass-Ceramics | 93 |
| 2.2.5.2 | Enstatite Glass-Ceramics | 97 |
| 2.2.5.3 | Forsterite Glass-Ceramics | 99 |
| 2.2.6 | SiO ₂ –Al ₂ O ₃ –CaO (Wollastonite) | 101 |
| 2.2.7 | SiO ₂ –Al ₂ O ₃ –ZnO (Zn-Stuffed β-Quartz, Willemite-Zincite) | 103 |
| 2.2.7.1 | Zinc-Stuffed β-Quartz Glass-Ceramics | 103 |
| 2.2.7.2 | Willemite and Zincite Glass-Ceramics | 105 |
| 2.2.8 | SiO ₂ –Al ₂ O ₃ –ZnO–MgO (Spinel, Gahnite) | 105 |
| 2.2.8.1 | Spinel Glass-Ceramic without β-Quartz | 105 |
| 2.2.8.2 | β-Quartz-Spinel Glass-Ceramics | 107 |
| 2.2.9 | SiO ₂ –Al ₂ O ₃ –CaO (Slag Sital) | 108 |
| 2.2.10 | SiO ₂ –Al ₂ O ₃ –K ₂ O (Leucite) | 111 |
| 2.2.11 | SiO ₂ –Ga ₂ O ₃ –Al ₂ O ₃ –Li ₂ O–Na ₂ O–K ₂ O (Li–Al–Gallate Spinel) | 114 |
| 2.2.12 | SiO ₂ –Al ₂ O ₃ –SrO–BaO (Sr–Feldspar–Celsian) | 115 |
| 2.3 | Fluorosilicates | 118 |
| 2.3.1 | SiO ₂ –(R ³⁺) ₂ O ₃ –MgO–(R ²⁺)O–(R ⁺) ₂ O–F (Mica) | 118 |
| 2.3.1.1 | Alkaline Phlogopite Glass-Ceramics | 119 |
| 2.3.1.2 | Alkali-Free Phlogopite Glass-Ceramics | 124 |
| 2.3.1.3 | Tetrasilicic Mica Glass-Ceramic | 125 |
| 2.3.2 | SiO ₂ –Al ₂ O ₃ –MgO–CaO–ZrO ₂ –F (Mica, Zirconia) | 126 |
| 2.3.3 | SiO ₂ –CaO–R ₂ O–F (Canasite) | 128 |

| | | |
|---------|---|-----|
| 2.3.4 | SiO ₂ –MgO–CaO–(R ⁺) ₂ O–F (Amphibole) | 132 |
| 2.4 | Silicophosphates | 136 |
| 2.4.1 | SiO ₂ –CaO–Na ₂ O–P ₂ O ₅ (Apatite) | 136 |
| 2.4.2 | SiO ₂ –MgO–CaO–P ₂ O ₅ –F (Apatite, Wollastonite) | 137 |
| 2.4.3 | SiO ₂ –MgO–Na ₂ O–K ₂ O–CaO–P ₂ O ₅ (Apatite) | 138 |
| 2.4.4 | SiO ₂ –Al ₂ O ₃ –MgO–CaO–Na ₂ O–K ₂ O–P ₂ O ₅ –F (Mica, Apatite) | 139 |
| 2.4.5 | SiO ₂ –MgO–CaO–TiO ₂ –P ₂ O ₅ (Apatite, Magnesium Titanate) | 143 |
| 2.4.6 | SiO ₂ –Al ₂ O ₃ –CaO–Na ₂ O–K ₂ O–P ₂ O ₅ –F (Needlelike Apatite) | 144 |
| 2.4.6.1 | Formation of Needlelike Apatite as a Parallel Reaction to Rhenanite | 147 |
| 2.4.6.2 | Formation of Needlelike Apatite from Disordered Spherical Fluoroapatite | 151 |
| 2.4.7 | SiO ₂ –Al ₂ O ₃ –CaO–Na ₂ O–K ₂ O–P ₂ O ₅ –F/Y ₂ O ₃ , B ₂ O ₃ (Apatite and Leucite) | 152 |
| 2.4.7.1 | Fluoroapatite and Leucite | 152 |
| 2.4.7.2 | Silicate Oxyapatite and Leucite | 153 |
| 2.4.8 | SiO ₂ –CaO–Na ₂ O–P ₂ O ₅ –F (Rhenanite) | 156 |
| 2.5 | Iron Silicates | 158 |
| 2.5.1 | SiO ₂ –Fe ₂ O ₃ –CaO | 158 |
| 2.5.2 | SiO ₂ –Al ₂ O ₃ –FeO–Fe ₂ O ₃ –K ₂ O (Mica, Ferrite) | 159 |
| 2.5.3 | SiO ₂ –Al ₂ O ₃ –Fe ₂ O ₃ –(R ⁺) ₂ O–(R ²⁺)O (Basalt) | 160 |
| 2.6 | Phosphates | 163 |
| 2.6.1 | P ₂ O ₅ –CaO (Metaphosphates) | 163 |
| 2.6.2 | P ₂ O ₅ –CaO–TiO ₂ | 166 |
| 2.6.3 | P ₂ O ₅ –Na ₂ O–BaO and P ₂ O ₅ –TiO ₂ –WO ₃ | 167 |
| 2.6.3.1 | P ₂ O ₅ –Na ₂ O–BaO System | 167 |
| 2.6.3.2 | P ₂ O ₅ –TiO ₂ –WO ₃ System | 167 |
| 2.6.4 | P ₂ O ₅ –Al ₂ O ₃ –CaO (Apatite) | 167 |
| 2.6.5 | P ₂ O ₅ –B ₂ O ₃ –SiO ₂ | 169 |
| 2.6.6 | P ₂ O ₅ –SiO ₂ –Li ₂ O–ZrO ₂ | 170 |
| 2.6.6.1 | Glass-Ceramics Containing 16 wt% ZrO ₂ | 171 |
| 2.6.6.2 | Glass-Ceramics Containing 20 wt% ZrO ₂ | 171 |
| 2.6.7 | P ₂ O ₅ –FeO–Na ₂ O (Pyrophosphate) | 174 |
| 2.7 | Ion Exchange in Glass-Ceramics | 174 |
| 2.8 | Rare Earth-Doped Light-Transmitting Glass-Ceramics | 186 |
| 2.8.1 | Ce:YAG Glass-Ceramics for White LEDs | 186 |
| 2.8.2 | Eu, Dy: SrAl ₂ O ₄ Transparent Glass-Ceramics with Long Phosphorescence and High Brightness | 188 |
| 2.8.3 | Eu ²⁺ -Activated β-Ca ₂ SiO ₄ and Ca ₃ Si ₂ O ₇ Green and Red Phosphors for White LEDs | 191 |
| 2.8.4 | Transparent (Er, Yb)NbO ₄ -β-Quartz Solid Solution Glass-Ceramics | 193 |
| 2.9 | Extension of Glass-Ceramic Systems Developed on the Basis of Multifold Nucleation and Crystallization Mechanisms | 193 |
| 2.9.1 | Sr-apatite–Leucite/Pollucite/Rb-leucite | 194 |
| 2.9.1.1 | Internal Nucleation and Crystallization | 194 |
| 2.9.1.2 | Internal Mechanisms Combined with Surface Nucleation and Crystallization | 195 |
| 2.9.2 | Lithium Disilicate–Apatite Glass-Ceramic | 197 |
| 2.9.3 | Lithium Disilicate and Cesium Aluminosilicate Glass-Ceramics | 203 |
| 2.9.4 | Lithium Disilicate–Diopside/Wollastonite Glass-Ceramic | 205 |
| 2.9.5 | Lithium Disilicate–Niobate/Tantalate Glass-Ceramic | 207 |
| 2.9.6 | Quartz–Lithium Disilicate Glass-Ceramic | 207 |
| 2.9.7 | Transparent Glass-Ceramics Based on Lithium Disilicate and Petalite | 209 |

| | | |
|----------|---|------------|
| 2.10 | Other Systems | 210 |
| 2.10.1 | Perovskite-Type Glass-Ceramics | 210 |
| 2.10.1.1 | $\text{SiO}_2\text{-Nb}_2\text{O}_5\text{-Na}_2\text{O-(BaO)}$ | 210 |
| 2.10.1.2 | $\text{SiO}_2\text{-Al}_2\text{O}_3\text{-TiO}_2\text{-PbO}$ | 211 |
| 2.10.1.3 | $\text{SiO}_2\text{-Al}_2\text{O}_3\text{-K}_2\text{O-Ta}_2\text{O}_5\text{-Nb}_2\text{O}_5$ | 212 |
| 2.10.2 | $\text{SiO}_2\text{-B}_2\text{O}_3\text{-TiO}_2\text{-La}_2\text{O}_3$ System | 213 |
| 2.10.3 | Transparent and Highly Crystalline BaAl_4O_7 Glass-Ceramics | 213 |
| 2.10.4 | Chalcogenide Glass-Ceramics | 214 |
| 2.10.5 | Ilmenite-Type ($\text{SiO}_2\text{-Al}_2\text{O}_3\text{-Li}_2\text{O-Ta}_2\text{O}_5$) Glass-Ceramics | 214 |
| 2.10.6 | $\text{B}_2\text{O}_3\text{-BaFe}_{12}\text{O}_{19}$ (Barium Hexaferrite) or ($\text{BaFe}_{10}\text{O}_{15}$) Barium Ferrite | 214 |
| 2.10.7 | $\text{SiO}_2\text{-Al}_2\text{O}_3\text{-BaO-TiO}_2$ (Barium Titanate) | 215 |
| 2.10.8 | $\text{Bi}_2\text{O}_3\text{-SrO-CaO-CuO}$ | 216 |
| 3 | Microstructure Control | 217 |
| 3.1 | Solid State Reactions | 217 |
| 3.1.1 | Isochemical Phase Transformation | 217 |
| 3.1.2 | Reactions Between Phases | 218 |
| 3.1.3 | Exsolution | 218 |
| 3.1.4 | Use of Phase Diagrams to Predict Glass-Ceramic Assemblages | 218 |
| 3.2 | Microstructure Design | 219 |
| 3.2.1 | Nanocrystalline Microstructures | 219 |
| 3.2.2 | Cellular Membrane Microstructures | 221 |
| 3.2.3 | Coast-and-Island Microstructure | 222 |
| 3.2.4 | Dendritic Microstructures | 225 |
| 3.2.5 | Relict Microstructures | 227 |
| 3.2.6 | House-of-Cards Microstructures | 228 |
| 3.2.6.1 | Nucleation Reactions | 229 |
| 3.2.6.2 | Primary Crystal Formation and Mica Precipitation | 229 |
| 3.2.7 | Cabbage-Head Microstructures | 229 |
| 3.2.8 | Acicular Interlocking Microstructures | 235 |
| 3.2.9 | Lamellar Twinned Microstructures | 237 |
| 3.2.10 | Preferred Crystal Orientation | 238 |
| 3.2.11 | Crystal Network Microstructures | 240 |
| 3.2.12 | Nature as an Example | 242 |
| 3.2.13 | Nanocrystals | 242 |
| 3.3 | Control of Key Properties | 243 |
| 3.3.1 | General | 243 |
| 3.3.2 | Multifold Nucleation and Crystallization | 245 |
| 3.3.2.1 | Control of Mechanical and Thermal Properties | 245 |
| 3.3.2.2 | Control of Optical and Thermal Properties | 245 |
| 3.3.2.3 | Control of Mechanical and Optical Properties | 246 |
| 3.3.2.4 | Control of Mechanical and Magnetic Properties | 246 |
| 3.3.2.5 | Control of Biological and Mechanical Properties | 246 |
| 3.4 | Methods and Measurements | 246 |
| 3.4.1 | Chemical System and Crystalline Phases | 246 |
| 3.4.2 | Determination of Crystal Phases | 247 |
| 3.4.3 | Kinetic Process of Crystal Formation | 249 |
| 3.4.4 | Determination of Microstructure | 252 |
| 3.4.5 | Mechanical, Optical, Electrical, Chemical, and Biological Properties | 252 |

- 3.4.5.1 Optical Properties and Chemical Composition of Glass-Ceramics 254
- 3.4.5.2 Mechanical Properties and Microstructure of Glass-Ceramics 254
- 3.4.5.3 Electrical Properties 256
- 3.4.5.4 Chemical Properties 256
- 3.4.5.5 Biological Properties 257

- 4 Applications of Glass-Ceramics 259**
- 4.1 Technical Applications 259
 - 4.1.1 Radomes 259
 - 4.1.2 Photosensitive and Etched Patterned Materials 259
 - 4.1.2.1 Fotoform[®] and Fotoceram[®] 259
 - 4.1.2.2 Foturan[®] 262
 - 4.1.2.3 Additional Products 265
 - 4.1.3 Machinable Glass-Ceramics 265
 - 4.1.3.1 MACOR[®] and DICOR[®] 265
 - 4.1.3.2 Vitronit[™] 268
 - 4.1.3.3 Photoveel[™] 269
 - 4.1.4 Magnetic Memory Disk Substrates 269
 - 4.1.5 Liquid Crystal Displays 273
- 4.2 Consumer Applications 273
 - 4.2.1 β -Spodumene Solid-Solution Glass-Ceramic 273
 - 4.2.2 β -Quartz Solid-Solution Glass-Ceramic 274
- 4.3 Optical Applications 279
 - 4.3.1 Telescope Mirrors 279
 - 4.3.1.1 Requirements for Their Development 279
 - 4.3.1.2 Zerodur[®] Glass-Ceramics 279
 - 4.3.2 Integrated Lens Arrays 281
 - 4.3.3 Applications for Luminescent Glass-Ceramics 283
 - 4.3.3.1 Cr-Doped Mullite for Solar Concentrators 283
 - 4.3.3.2 Cr-Doped Gahnite Spinel for Tunable Lasers and Optical Memory Media 286
 - 4.3.3.3 Rare-Earth Doped Oxyfluorides for Amplification, Upconversion, and Quantum Cutting 287
 - 4.3.3.4 Chromium (Cr^{4+})-Doped Forsterite, β -Willemite, and Other Orthosilicates for Broad Wavelength Amplification 293
 - 4.3.3.5 Ni^{2+} -Doped Gallate Spinel for Amplification and Broadband Infrared Sources 295
 - 4.3.3.6 YAG Glass-Ceramic Phosphor for White LED 300
- 4.3.4 Optical Components 300
 - 4.3.4.1 Glass-Ceramics for Fiber Bragg Grating Athermalization 300
 - 4.3.4.2 Laser-Induced Crystallization for Optical Gratings and Waveguides 306
 - 4.3.4.3 Glass-Ceramic Ferrule for Optical Connectors 307
 - 4.3.4.4 Applications for Transparent ZnO Glass-Ceramics with Controlled Infrared Absorbance and Microwave Susceptibility 308
- 4.4 Medical and Dental Glass-Ceramics 309
 - 4.4.1 Glass-Ceramics for Medical Applications 310
 - 4.4.1.1 CERABONE[®] 310
 - 4.4.1.2 CERAVITAL[®] 311
 - 4.4.1.3 BIOVERIT[®] 312
 - 4.4.2 Glass-Ceramics for Dental Restoration 313
 - 4.4.2.1 Moldable Glass-Ceramics for Metal-Free Dental Restorations 314

| | | |
|---------|--|-----|
| 4.4.2.2 | Machinable Glass-Ceramics | 324 |
| 4.4.2.3 | Fusion of Glass-Ceramics on High Toughness Sintered Ceramics | 332 |
| 4.4.2.4 | Leucite-Apatite Glass-ceramic on Metal Frameworks and Metal-Free Restorations | 335 |
| 4.5 | Electrical and Electronic Applications | 339 |
| 4.5.1 | Insulators | 339 |
| 4.5.2 | Electronic Packaging | 340 |
| 4.5.2.1 | Requirements for Their Development | 340 |
| 4.5.2.2 | Properties and Processing | 341 |
| 4.5.2.3 | Applications | 342 |
| 4.5.3 | Dielectric Glass-Ceramics for GHz Electronics | 343 |
| 4.6 | Architectural Applications | 345 |
| 4.7 | Coatings and Solders | 347 |
| 4.8 | Glass-Ceramics for Energy Applications | 348 |
| 4.8.1 | Glass-Ceramic Components for Batteries | 349 |
| 4.8.1.1 | Glass-Ceramics as Cathodes for Lithium or Sodium Ion Batteries and Glass as Anodes | 349 |
| 4.8.1.2 | Electrolytes | 349 |
| 4.8.2 | Joining Materials for Solid Oxide Fuel Cell Components | 350 |
| 4.9 | Application of Glass-Ceramic Principle to Functional Materials | 352 |
| 4.10 | Forming Processes for Glass-Ceramics | 352 |
| 4.10.1 | Pressing | 352 |
| 4.10.2 | Casting | 353 |
| 4.10.3 | Spinning (Centrifugal Casting) | 353 |
| 4.10.4 | Rolling | 354 |
| 4.10.5 | Float Process | 354 |
| 4.10.6 | Direct Forming or Reforming of Glass-Ceramics | 357 |

5 Future Directions 358

Appendix A: Twenty-one Figures of 23 Crystal Structures 360

References 381

Index 415

Introduction to the Third Edition

The main aims of the third edition of this reference book are to present research and development highlights since 2012, to update areas of fundamental importance to glass-ceramics like nucleation and growth, and to add material concerning forming processes, including parent glass forming, novel crystallization processes and ion exchange strengthening.

There have been major advances in products based on glass-ceramics in dentistry and other biomaterials. In this edition, a new approach has been chosen to present the materials for restorative dentistry: A particular focus is placed on illustrating the immediate benefits of these products to both dentists and patients. New scientific findings have made it possible to increase the processing efficiency of dental restorative materials and significantly extend their application range. Today, patients have a wide array of metal-free, inorganic biomaterials at their disposal, which offer both excellent function and aesthetics.

In this edition, new products and potential uses involving novel optical, electronic, and mechanical properties are described. These include transparent glass-ceramics for mobile phones and tablets, and translucent materials for LEDs and phosphorescent displays.

The third edition of this publication, like the first two, is a product of close collaboration between the two authors. They regularly consulted together on their individual sections. They discussed many aspects of composition, phase transformation, microstructure, and useful novel analytic techniques; the latter often used in combination to better understand the sequence of crystallization in various glass systems.

W. Höland would like to give special mention to the following people from Ivoclar Vivadent AG: Markus Rampf, Marc Dittmer, Christian Ritzberger, Marcel Schweiger, and Ronny Watzke for their scientific discussions and R. Ganley, V.M. Rheinberger and T. Hirt for their support to glass-ceramic research. He would also like to thank the TC 07 Subcommittee of the International Congress on Glass (ICG), and colleagues of this group, especially J. Deubener, M.J. Pascual, T. Komatsu, E.D. Zanotto, I. Mitra. A special Thanks goes to M. Höland (University of Applied Sciences, Buchs, SG, Switzerland) for many scientific discussions. S. Fuchs (South Africa) is thanked for translation work.

Both authors like to thank S. Tanabe, H. Hosono and J. Schmelzer who helped with valuable suggestions and advice.

G. Beall would like to thank Charlene Smith for her helpful comments and advice. He would also credit D.L. Morse, G. Calabrese, C. Heckle and M. Pambianchi for their continuing support of research on glass-ceramics at Corning Incorporated.

Both authors would also like to thank A. Höland (graphic design, Schaan, Liechtenstein) and M. Höland for graphs in the second and third edition of this textbook, and I. Heidelauf (Ivoclar-Vivadent AG) for the graphs of the first edition.

History

Glass-ceramics are ceramic materials formed through the controlled nucleation and crystallization of glass. Glasses are melted, fabricated to shape, and thermally converted to a predominantly crystalline ceramic. The basis of controlled internal crystallization lies in efficient nucleation that allows the development of fine, randomly oriented grains generally without voids, microcracks, or other porosity. The glass-ceramic process, therefore, is basically a simple thermal process as illustrated in Figure H.1.

It occurred to Reamur (1739) and to many people since that a dense ceramic made via the crystallization of glass objects would be highly desirable. It was not until about 35 years ago, however, that this idea was consummated. The invention of glass-ceramics took place in the mid-1950s by the famous glass chemist and inventor, Dr. S.D. Stookey. It is useful to examine the sequence of events leading to the discovery of these materials (Table H.1).

Dr. Stookey at the time was not primarily interested in ceramics. He was preoccupied in precipitating silver particles in glass in order to achieve a permanent photographic image. He was studying as host glasses lithium silicate compositions because he found he could chemically precipitate silver in alkali silicate glasses, and those containing lithium had the best chemical durability. In order to develop the silver particles, he normally heated glasses previously exposed to ultraviolet light just above their glass transition temperature at around 450 °C. One night the furnace accidentally overheated to 850 °C, and, on observation of the thermal recorder, he expected to find a melted pool of glass. Surprisingly, he observed a white material that had not changed shape. He immediately recognized as a ceramic produced showing no distortion from the original glass article. A second serendipitous event then occurred. He dropped the sample accidentally, and it sounded more like metal than glass. He then realized that the ceramic he had produced had unusual strength.

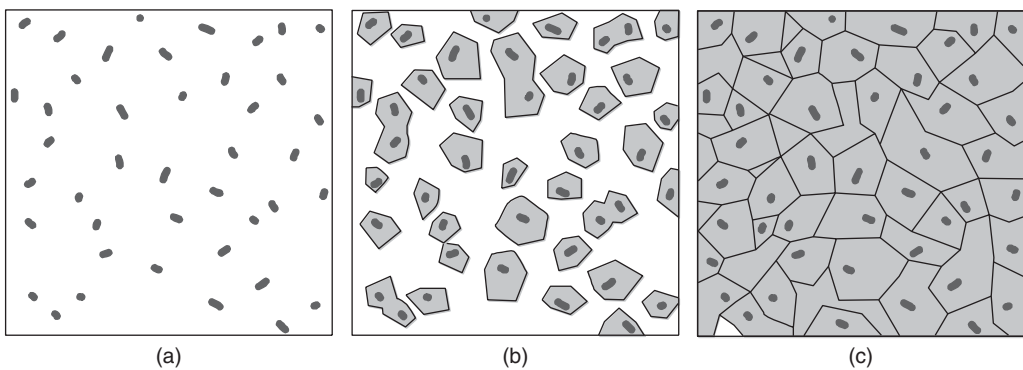


Figure H.1 From glass to glass-ceramic. (a) nuclei formation, (b) crystal growth on nuclei, and (c) glass-ceramic microstructure.

Table H.1 Invention of glass-ceramics (S.D. Stookey, 1950s).

-
- Photosensitive silver precipitation in $\text{Li}_2\text{O}-\text{SiO}_2$ glass; furnace *overheats*; $\text{Li}_2\text{Si}_2\text{O}_5$ crystallizes on Ag nuclei; first glass-ceramic
 - Sample *accidentally dropped*; unusual strength
 - Near-zero-thermal-expansion crystal phases described in $\text{Li}_2\text{O}-\text{Al}_2\text{O}_3-\text{SiO}_2$ system (Hummel, 1951, Roy 1959)
 - TiO_2 tried as nucleation agent based on its observed precipitation in *dense thermometer opals*
 - Aluminosilicate glass-ceramic (e.g. Corning Ware[®]) developed
-

On contemplating the significance of this unplanned experiment, Stookey recalled that lithium aluminosilicate crystals had been reported with very low thermal expansion characteristics; in particular, a phase, β -spodumene, had been described by Hummel (1951) as having a near-zero thermal expansion characteristic. He was well aware of the significance of even moderately low expansion crystals in permitting thermal shock in otherwise fragile ceramics. He realized if he could nucleate these and other low coefficient of thermal expansion phases in the same way as he had lithium disilicate, the discovery would be far more meaningful. Unfortunately, he soon found that silver or other colloidal metals are not effective in nucleation of these aluminosilicate crystals. Here he paused and relied on his personal experience with specialty glasses. He had at one point worked on dense thermometer opals. These are the white glasses that compose the dense, opaque stripe in a common thermometer. Historically, this effect had been developed by precipitation of crystals of high refractive index such as zinc sulfide or titania. He, therefore, tried adding titania as a nucleating agent in aluminosilicate glasses and discovered it to be amazingly effective. Strong and thermal shock-resistant glass-ceramics were then developed commercially within a year or two of this work with well-known products such as rocket nose cones and Corning Ware[®] cookware resulting (Stookey 1959).

In Summary, a broad materials advance had been achieved from a mixture of serendipitous events controlled by chance and good exploratory research related to a practical concept, albeit unrelated to a specific vision of any of the eventual products. Knowledge of the literature, good observation skills, and deductive reasoning were clearly evident in allowing the chance events to bear fruit.

Without the internal nucleation process as a precursor to crystallization, devitrification is initiated at lower-energy surface sites. As Reamur was painfully aware, the result is an ice-cube-like structure (Figure H.2), where the surface-oriented crystals meet in a plane of weakness. Flow of the uncrystallized core glass in response to changes in bulk density during crystallization commonly forces the original shape to undergo grotesque distortions. On the other hand, because crystallization can occur uniformly and at high viscosities, internally nucleated glasses can undergo the transformation from glass to ceramic with little or no deviation from the original shape.

To consider the advantages of glass-ceramics over their parent glasses, one must consider the unique features of crystals, beginning with their ordered structure. When crystals meet, structural discontinuities or grain boundaries are produced. Unlike glasses, crystals also have discrete structural plans that may cause deflection, branching, or splintering of cracks. Thus the presence of cleavage planes and grain boundaries serves to act as an impediment for fracture propagation. This accounts for the better mechanical reliability of finely crystallized glasses. In addition, the spectrum of properties in crystals is very broad compared with that of glasses. Thus some crystals may have extremely low or even negative thermal expansion behavior. Others, like sapphire, may be harder than any glass, and crystals like mica might be extremely soft. Certain crystalline families also may have unusual luminescent, dielectric,

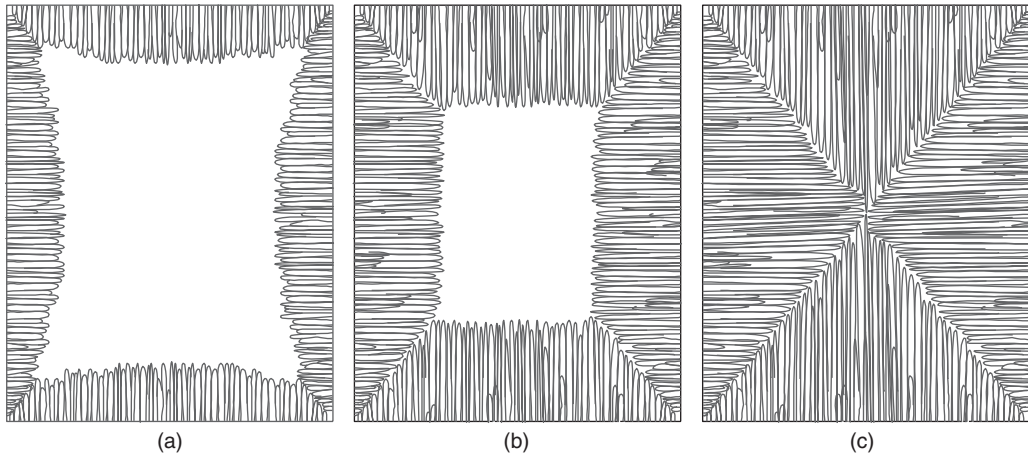


Figure H.2 Crystallization of glass without internal nucleation.

or magnetic properties. Some are semiconducting or even, as recent advances attest, may be superconducting at liquid nitrogen temperatures. In addition, if crystals can be oriented, polar properties like piezoelectricity or optical polarization may be induced.

Another method of manufacture of glass-ceramics has proven technically and commercially viable. This involves the sintering and crystallization of powdered glass. This approach has certain advantages over body-crystallized glass-ceramics. First, traditional glass-ceramic processes may be used, e.g. slip casting, pressing, and extruding. Second, because of the high flow rates before crystallization, glass-ceramic coatings on metals or other ceramics may be applied by using this process. Finally, and most important, is the ability to use surface imperfections in quenched frit as nucleation sites. This process typically involves milling a quenched glass into fine 3–15 μm particle diameter particulate. This powder is then formed by conventional ceramming called forming techniques in viscous sintering to full density just before the crystallization process is completed. Figure H.3 shows transformation of a powdered glass compact (Figure H.3a) to a dense sintered glass with some surface nucleation sites (Figure H.3b) and finally to a highly crystalline frit derived glass-ceramic (Figure H.3c). Note the similarity in structure between the internally nucleated glass-ceramic in Figure H.1c. The first commercial exploitation of frit-derived glass-ceramics was the devitrifying frit solder glasses for sealing television bulbs. The technology has been applied to cofired, multilayer substrates for electronic packaging and biomaterials for dental restoration.

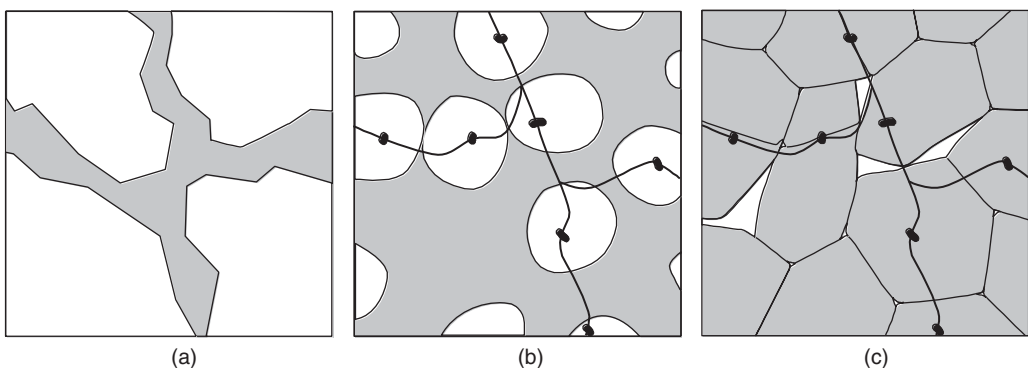


Figure H.3 Glass-ceramics from powdered glass. (a) powdered glass compact, (b) densification and incipient crystallization, and (c) frit-derived glass-ceramic.

1

Principles of Designing Glass-Ceramic Formation

1.1 Advantages of Glass-Ceramic Formation

Glass-ceramics have been shown to feature favorable thermal, chemical, biological, and dielectric properties, generally superior to metals and organic polymers in these areas. Moreover, glass-ceramics also demonstrate considerable advantages over inorganic materials, such as glasses and ceramics. The large variety of compositions and the possibility of developing special microstructures should be noted in particular. It goes without saying that these advantageous properties assure the favorable characteristics of the glass-ceramic end products.

As the name clearly indicates, glass-ceramics are classified between inorganic glasses and ceramics. A glass-ceramic may be highly crystalline or may contain substantial residual glass. It is composed of one or more glassy and crystalline phases. The glass-ceramic is produced from a base glass by controlled crystallization. The new crystals produced in this way grow directly in the glass phase, and at the same time slowly change the composition of the remaining glass.

The synthesis of the base glass represents an important step in the development of glass-ceramic materials. Many different ways of traditional melting and forming, as well as sol-gel, chemical vapor deposition, and other means of production of the base glasses are possible. Although the development of glass-ceramics is complicated and time consuming, the wide spectrum of their chemical synthesis is useful for achieving different properties.

The most important advantage of the glass-ceramic formation, however, is the wide variety of special microstructures. Most types of microstructures that form in glass-ceramics cannot be produced in any other material. The glass phases may themselves demonstrate different structures. Furthermore, they may be arranged in the microstructure in different morphological ways. Crystal phases possess an even wider variety of characteristics. They may demonstrate special morphologies related to their particular structures, as well as considerable differences in appearance depending on their mode of growth. All these different ways of forming microstructures involve controlled nucleation and crystallization, as well as the choice of parent glass composition.

Glass-ceramics demonstrating particularly favorable properties were developed on the basis of these two key advantages, that is, the variation of the chemical composition and of the microstructure. These properties are listed in Tables 1.1 and 1.2 and are briefly outlined in the following sections.

1.1.1 Processing Properties

The research on the discovery of suitable base glasses revealed that the technology used in the primary shaping of glass could also be applied to glass-ceramics. Therefore, bulk glasses

Table 1.1 Particularly favorable properties of glass-ceramics.

Processing properties

Rolling, casting, pressing, spin, casting, press-and-blow method, and drawing are possible

Limited and controllable shrinkage

No porosity in monolithic glass-ceramics

Thermal properties

Expansion can be controlled as desired, depending on the temperature, with zero or even negative expansion being coefficient of thermal expansion possible

High temperature stability

Optical properties

Translucency or opacity

Photoinduction is possible

Pigmentation

Opalescence, fluorescence

Chemical properties

Resorbability or high chemical durability

Biological properties

Biocompatibility

Bioactivity

Mechanical properties

Machinability

High strength and toughness

Electrical and magnetic properties

Isolation capabilities (low dielectric constant and loss of high resistivity and breakdown voltage)

Ion conductivity and superconductivity

Ferromagnetism

Table 1.2 Particularly favorable combinations of properties of glass-ceramics (selection).

- Mechanical property (machinability) + thermal properties (temperature resistance)
 - Thermal property (zero expansion + temperature resistance) + chemical durability
 - Mechanical property (strength) + optical property (translucency) + favorable processing properties
 - Strength + translucency + biological properties + favorable processing properties
-

are produced by rolling, pressing, casting, spin casting, or by press-blowing a glass melt or by drawing a glass rod or ring from the melt. The thin-layer method is also used to produce thin glass sheets, for example. In addition, glass powder or grains are transformed into glass-ceramics.

1.1.2 Thermal Properties

A particular advantage in the production of glass-ceramics is that products demonstrating almost zero shrinkage can be produced. These specific materials are produced on a large scale for industrial, technological, and domestic applications (e.g. kitchenware).

1.1.3 Optical Properties

Since glass-ceramics are nonporous and usually contain a glass phase, they demonstrate a high level of translucency and in some cases even high transparency. Furthermore, it is also possible to produce very opaque glass-ceramics, depending on the type of crystal and the microstructure of the material. Glass-ceramics can be produced in virtually every color. In addition, photo-induced processes may be used to produce glass-ceramics and to shape high-precision and patterned end products.

Fluorescence, both visible and infrared, and opalescence in glass-ceramics are also important optical characteristics.

1.1.4 Chemical Properties

Chemical properties, ranging from resorbability to chemical durability, can be controlled according to the nature of the crystal, the glass phase, or the nature of the interface between the crystal and the glass phase. As a result, resorbable or chemically durable glass-ceramics can be produced. The microstructure in particular also permits the combination of resorbability of one phase and chemical durability of the other phase.

1.1.5 Biological Properties

Biocompatible and durable glass-ceramics have been developed for human medicine and for dentistry in particular. Furthermore, bioactive materials are used in implantology.

1.1.6 Mechanical Properties

Although the highest flexural strength values measured for metal alloys have not yet been achieved in glass-ceramics, it has been possible to achieve flexural strengths of up to 500 MPa. The toughness of glass-ceramics has also been considerably increased over the years. As a result, K_{IC} values of more than $3 \text{ MPa}\cdot\text{m}^{0.5}$ have been reached. No other material demonstrates these properties together with translucency and allows itself to be pressed or cast, without shrinking or pores developing, as in the case of monolithic glass-ceramics.

The fact that glass-ceramics can be produced as machinable materials represents an additional advantage. In other words, by first processing the glass melt, a primary shape is given to the material. Next, the glass-ceramic is provided with a relatively simple final shape by drilling, milling, grinding, or sawing. Furthermore, the surface characteristics of glass-ceramics, for example roughness, polishability, luster, or abrasion behavior, can also be controlled.

1.1.7 Electrical and Magnetic Properties

Glass-ceramics with special electrical or magnetic properties can also be produced. The electrical properties are particularly important if the material is used for isolators in the electronics or micro-electronics industries. It must also be noted that useful composites can be formed by combining glass-ceramics with other materials, for example metal. In addition, glass-ceramics demonstrating high ion conductivity and even superconductivity have been developed. Furthermore, magnetic properties in glass-ceramics were produced similarly to those in sintered ceramics. These materials are processed according to methods involving primary shaping of the base glasses followed by thermal treatment for crystallization.

Table 1.3 Glass-ceramic design.*Composition*

- Bulk chemical
Glass formation and workability
Internal or surface nucleation
- Phase assemblage
General physical and chemical characteristics

Microstructure

- Key to mechanical and optical properties
- Can promote or diminish characteristics of key phase

1.2 Factors of Design

In the design of glass-ceramics, the two most important factors are composition and microstructure (Table 1.3). The bulk chemical composition controls the ability to form a glass and determines its degree of workability. It also determines whether internal or surface nucleation can be achieved. If internal nucleation is desired, as is the case when hot glass forming of articles, appropriate nucleating agents are melted into the glass as part of the bulk composition. The bulk composition also directly determines the potential crystalline assemblage, and this in turn determines the general physical and chemical characteristics, for example hardness, density, thermal expansion coefficient, and acid resistance.

Microstructure is of equal importance to composition. This feature is the key to most mechanical and optical properties, and it can promote or diminish the characteristics of key crystals in glass-ceramics. It is clear that microstructure is not an independent variable. It obviously depends on the bulk composition and crystalline phase assemblage, and it also can be modified, often dramatically, by varying the thermal treatment.

1.3 Crystal Structures and Mineral Properties

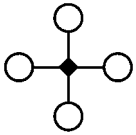
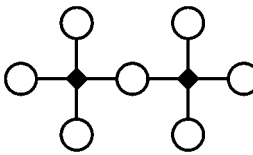
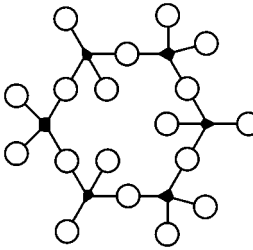
Since the most important glass-forming systems are based on silicate compositions, the key crystalline components of glass-ceramics are therefore silicates. Certain oxide minerals, however, are important, both in controlling nucleation, as well as forming accessory phases in the final product.

1.3.1 Crystalline Silicates

Crystalline silicates of interest in glass-ceramic materials can be divided into six groups according to the degree of polymerization of the basic tetrahedral building blocks. These are generally classified as follows (Tables 1.4 and 1.5):

- nesosilicates (independent $(\text{SiO}_4)^{4-}$ tetrahedra);
- sorosilicates (based on $(\text{Si}_2\text{O}_7)^{6-}$ dimers);
- cyclosilicates (containing six-membered $(\text{Si}_6\text{O}_{18})^{12-}$ or $(\text{AlSi}_5\text{O}_{18})^{13-}$ rings);
- inosilicates (containing chains based on $(\text{SiO}_3)^{2-}$ single, $(\text{Si}_4\text{O}_{11})^{6-}$ double, or multiple);

Table 1.4 Structural classification of silicates found in glass-ceramics.

| | | | |
|------------------------------|-------------|--|---|
| Nesosilicates | | | |
| Isolated tetrahedra | | |  |
| 1 : 4 ratio of Si:O | 0% sharing | | |
| Forsterite $Mg_2(SiO_4)$ | | | |
| Sorosilicates | | | |
| Tetrahedral pairs | | |  |
| 2 : 7 ratio of Si:O | 25% sharing | | |
| Thortveitite $Sc_2(Si_2O_7)$ | | | |
| Cyclosilicates | | | |
| Ring silicates | | |  |
| 1 : 3 ratio of Si:O | 50% sharing | | |
| Beryl $Be_3Al_2(Si_6O_{18})$ | | | |

- phyllosilicates (sheet structures based on hexagonal layers of $(Si_4O_{10})^{4-}$, $(AlSi_3O_{10})^{5-}$, or $(Al_2Si_2O_{10})^{6-}$); and
- tectosilicates (frameworks of corner shared tetrahedra with formula SiO_2 , $(AlSi_3O_8)^{1-}$ or $(Al_2Si_2O_8)^{2-}$).

1.3.1.1 Nesosilicates

This is the least important mineral group in glass-ceramic technology because the low polymerization of silica in these minerals does not allow glass formation at these stoichiometries (Si:O ratio = 1 : 4). Nevertheless, such phases as forsterite (Mg_2SiO_4) and willemite (Zn_2SiO_4) can occur as minor phases. Willemite, in particular, when doped with Mn^{2+} , can create a strong green fluorescence even when present in small volume percents. Humite minerals, such as chondrodite ($Mg_2SiO_4 \cdot 2MgF_2$) and norbergite ($Mg_2SiO_4 \cdot MgF_2$), are precursor phases in some fluoromica glass-ceramics.

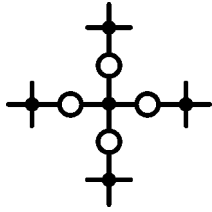

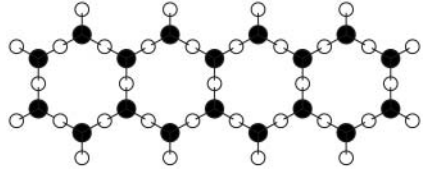
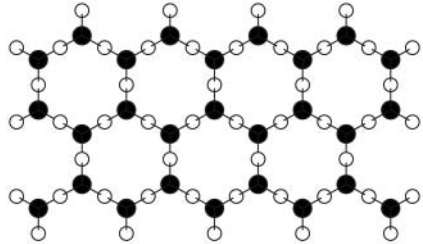
1.3.1.2 Sorosilicates

As is the case of the nesosilicates, sorosilicates are not glass-forming minerals because of their low Si:O ratio, namely 2 : 7. Again, they are sometimes present as minor phases in slag-based glass-ceramics, as in the case of the melilite crystal akermanite $Ca_2MgSi_2O_7$, and its solid-solution end member gehlenite $Ca_2Al_2SiO_7$. The latter contains a tetrahedrally coordinated Al^{3+} ion replacing one Si^{4+} ion.

1.3.1.3 Cyclosilicates

This group, often called ring silicates, is characterized by six-membered rings of (SiO_4) and (AlO_4) tetrahedral units, which are strongly cross-linked. They are best represented in glass-ceramic technology by the important phase cordierite: $Mg_2Al_4Si_5O_{18}$, which forms a glass, albeit a somewhat unstable or quite fragile one. Because the cyclosilicates are morphologically

Table 1.5 Structural classification of silicates found in glass-ceramics.

| | | |
|--|---------------|---|
| Inosilicates | | |
| Single-chain silicate (pyroxenes) 1 : 3 ratio of Si:O (infinite ring) Enstatite MgSiO_3 | 50% sharing |  |
| Double-chain silicates (amphiboles) 4 : 11 ratio of Si:O Tremolite $\text{Ca}_2\text{Mg}_5(\text{Si}_4\text{O}_{11})(\text{OH})_2$ | 62.5% sharing |  |
| Phyllosilicates | | |
| Layer silicates (micas and clays) 2 : 5 ratio of Si:O Kaolinite (china clay) $\text{Al}_2(\text{Si}_2\text{O}_5)(\text{OH})_4$ Muscovite (mica) $\text{KAl}_2(\text{AlSi}_3\text{O}_{10})(\text{OH})_2$ | 75% sharing |  |
| Tectosilicates | | |
| Network silicates (silica and feldspars) 1 : 2 ratio of Si:O Quartz SiO_2 Orthoclase $\text{K}(\text{AlSi}_3\text{O}_8)$ Anorthite $\text{Ca}(\text{Al}_2\text{Si}_2\text{O}_8)$ | 100% sharing |  |

Note that Al^{3+} sometimes substitutes for Si^{4+} in tetrahedral sites, but never more than 50%. Silicates tend to cleave between the silicate groups, leaving the strong Si—O bonds intact. Amphiboles cleave in fibers, micas into sheets.

similar to the tectosilicates and show important similarities in physical properties, they will both be included in Section “Structure Property Relationships in Ring Silicates.”

1.3.1.4 Inosilicates

Inosilicates, or chain silicates, as they are commonly referred to, are marginal glass-forming compositions with an Si:O ratio of 1 : 3 in the case of single chains and 4 : 11 in the case of double chains. They are major crystalline phases in some glass-ceramics known for high strength and fracture toughness. This is because the unidirectional backbone of tetrahedral silica linkage (see Table 1.5) often manifests itself in acicular or rodlike crystals that provide reinforcement to the glass-ceramic. Also, strong cleavage or twinning provides an energy-absorbing mechanism for advancing fractures.

Among the single-chain silicates of importance in glass-ceramics are enstatite (MgSiO_3), diopside ($\text{CaMgSi}_2\text{O}_6$), and wollastonite (CaSiO_3). These structures are depicted in Appendix Figures A7–A9. All three phases are normally monoclinic ($2/m$) as found in glass-ceramics, although enstatite can occur in the quenched orthorhombic form (protoenstatite), and wollastonite may be triclinic. Lamellar twinning and associated cleavage on the (100) plane are

key to the toughness of enstatite, while elongated crystals aid in the increase of glass-ceramic strength where wollastonite is a major phase (see Chapter 2).

Amphiboles are a class of double-chain silicates common as rock-forming minerals. Certain fluoroamphiboles, particularly potassium fluororichterite of stoichiometry $(\text{KNaCaMg}_5\text{Si}_8\text{O}_{22}\text{F}_2)$, can be crystallized from glasses of composition slightly modified with excess Al_2O_3 and SiO_2 . The resulting strong glass-ceramics display an acicular microstructure dominated by rods of potassium fluororichterite of aspect ratio greater than 10. The monoclinic ($2/m$) structure of this crystal is shown in Appendix Figure A10. Note the double chain $(\text{Si}_4\text{O}_{11})^{6-}$ backbone parallel to the c -axis.

Certain multiple chain silicates are good glass formers, because of even higher states of polymerization, with Si:O ratios of 2 : 5. These include fluorocanasite $(\text{K}_2\text{Na}_4\text{Ca}_5\text{Si}_{12}\text{O}_{30}\text{F}_4)$ and agrellite $(\text{NaCa}_2\text{Si}_4\text{O}_{10}\text{F})$. Both are nucleated directly by precipitation of the CaF_2 inherent in their composition. Both yield strong and tough glass-ceramics with intersecting bladed crystals. Canasite, in particular, produces glass-ceramics of exceptional mechanical resistance, largely because of the splintering effect of well-developed cleavage. Canasite has a fourfold box or tubelike backbone. Canasite is believed monoclinic (m), while agrellite is triclinic.

1.3.1.5 Phyllosilicates

Sheet silicates, or phyllosilicates, are layered phases with infinite two-dimensional hexagonal arrays of silica and alumina tetrahedra $(\text{Si}_2\text{O}_5)^{2-}$, $(\text{AlSi}_3\text{O}_{10})^{5-}$, or $(\text{Al}_2\text{Si}_2\text{O}_{10})^{6-}$. The simplest glass-ceramic crystals of this type are lithium and barium disilicate $(\text{Li}_2\text{Si}_2\text{O}_5, \text{BaSi}_2\text{O}_5)$, both of which form glasses (Si:O = 2 : 5) and are easily converted to glass-ceramics. The structure of orthorhombic $\text{Li}_2\text{Si}_2\text{O}_5$ involves corrugated sheets of $(\text{Si}_2\text{O}_5)^{2-}$ on the (010) plane (Appendix Figure A12). Lithium silicate glass-ceramics are easily melted and crystallized, and because of an interlocking tabular or lathlike form related to the layered structure, they show good mechanical properties.

Chemically more complex but structurally composed of simpler flat layers are the fluoromicas, the key crystals allowing machinability in glass-ceramics. The most common phase is fluorophlogopite $(\text{KMg}_3\text{AlSi}_3\text{O}_{10}\text{F}_2)$, which similar to most micas shows excellent cleavage on the basal plane (001). This crystal is monoclinic ($2/m$), although pseudo-hexagonal in appearance. It features thin laminae formed by the basal cleavage, which are flexible, elastic, and tough. Because of the high MgO and F content, this mica does not itself form a glass, but a stable glass can easily be made with B_2O_3 , Al_2O_3 , and SiO_2 additions. Other fluoromica stoichiometries of glass-ceramic interest include $\text{KMg}_{2.5}\text{Si}_4\text{O}_{10}\text{F}_2$, $\text{NaMg}_3\text{AlSi}_3\text{O}_{10}\text{F}_2$, $\text{Ba}_{0.5}\text{Mg}_3\text{AlSi}_3\text{O}_{10}\text{F}_2$, and the more brittle mica $\text{BaMg}_3\text{Al}_2\text{Si}_2\text{O}_{10}\text{F}_2$.

The structure of fluorophlogopite is shown in Appendix Figure A13. The individual layers are composed of three components, two $(\text{AlSi}_3\text{O}_{10})^{5-}$ tetrahedral sheets with hexagonal arrays of tetrahedra pointing inward toward an edge-sharing octahedral sheet composed of $(\text{MgO}_4\text{F}_2)^{8-}$ units. This T–O–T complex sheet is separated from the neighboring similar sheet by 12-coordinated potassium ions. This weak K–O bonding is responsible for the excellent cleavage on the (001) plane.

1.3.1.6 Tectosilicates

Framework silicates, also referred to as tectosilicates, are characterized by a tetrahedral ion-to-oxygen ratio of 1 : 2. The typical tetrahedral ions are silicon and aluminum, but, in some cases, germanium, titanium, boron, gallium, beryllium, magnesium, and zinc may substitute in these tetrahedral sites. All tetrahedral ions are typically bonded through oxygen to another tetrahedral ion. Silicon normally composes from 50% to 100% of the tetrahedral ions.

Framework silicates are the major mineral building blocks of glass-ceramics. Because these crystals are high in SiO_2 and Al_2O_3 , key glass-forming oxides, they are almost always good glass formers, thus satisfying the first requirement for glass-ceramic production. In addition, important properties such as low coefficient of thermal expansion (CTE), good chemical durability, and refractoriness are often associated with this family of crystals. Finally, certain oxide nucleating agents such as TiO_2 and ZrO_2 are only partially soluble in viscous melts corresponding to these highly polymerized silicates, and their solubility is a strong function of temperature. These factors allow exceptional nucleation efficiency to be achieved with these oxides in framework silicate glasses.

Silica Polymorphs The low-pressure silica polymorphs include quartz, tridymite, and cristobalite. The stable phase at room temperature is α -quartz or low quartz. This transforms to β -quartz or high quartz at approximately 573°C at 1 bar. The transition from β -quartz to tridymite occurs at 867°C and tridymite inverts to β -cristobalite at 1470°C . β -Cristobalite melts to silica liquid at 1727°C . All three of these stable silica polymorphs experience displacive transformations that involve structural contraction with decreased temperature, and all can be cooled stably or metastably to room temperature in glass-ceramics compositions (Heany 1994).

Quartz. The topological confirmation of the silica framework for α - and β -quartz is well known and is shown in Figure 1.1. The structure of α -quartz is easily envisioned as a distortion of of

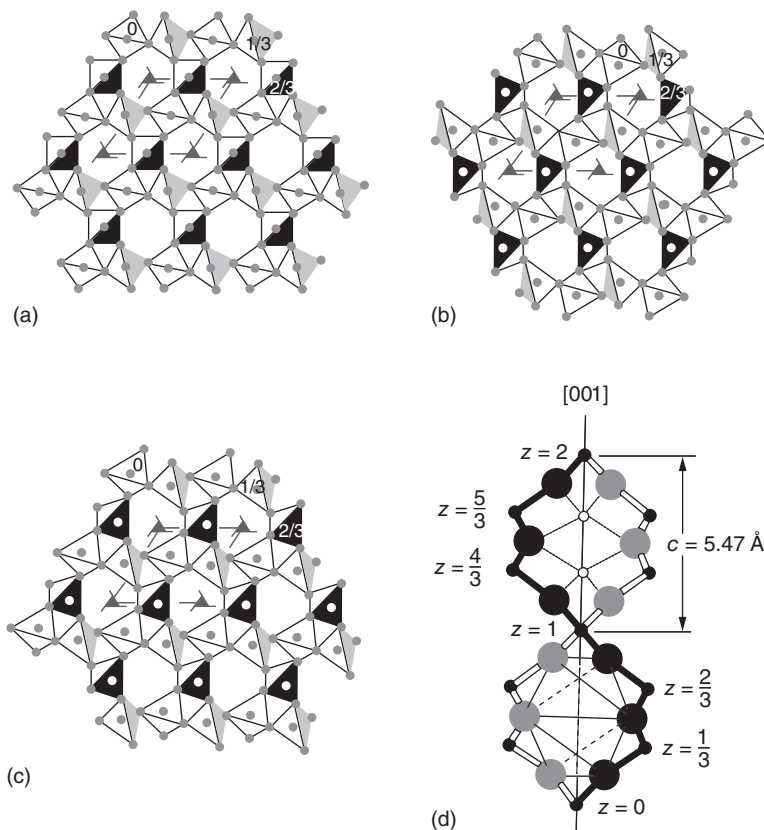


Figure 1.1 Projections of (a) β -quartz and (b) α -quartz and (c) along the c -axis. Both obverse (b) and reverse (c) settings are shown. The double helix structure of β -quartz is shown in panel (d).

the high-temperature beta modification. In high quartz, paired helical chains of silica tetrahedra spiral in the same sense around hexagonal screw axes parallel to the c -axis (Figure 1.1a). The intertwined chains produce open channels parallel to the c -axis that appear hexagonal in projection. The β -quartz framework contains six- and eight-membered rings with irregular shapes, and the space group is $P6_422$ or $P6_222$ depending on the chirality or handedness. When β -quartz is cooled below 573°C , the expanded framework collapses to the denser α -quartz configuration (Figure 1.1a,b). The structural data for α - and β -quartz is shown in Table 1.6. The thermal expansion of α -quartz from 0 to 300°C is approximately $15.0 \times 10^{-6}/\text{K}$. In its region of thermal stability, the thermal expansion coefficient of β -quartz is about $-0.5 \times 10^{-6}/\text{K}$. Unfortunately, the β -quartz structure cannot be quenched. Therefore, pure quartz in glass-ceramics undergoes rapid shrinkage on cooling below its transformation temperature. Since α -quartz is the densest polymorph of silica stable at room pressure, $\rho = 2.65 \text{ g/cm}^3$, it tends to impart high hardness to a glass-ceramic material.

Tridymite. In his classical effort to determine phase equilibria relationships among the silica polymorphs, Fenner (1913) observed that tridymite could be synthesized only with the aid of a “mineralizing agent” or flux, such as Na_2WO_4 . If pure quartz is heated, it bypasses tridymite and transforms directly to cristobalite at approximately 1050°C . A large variability in powder X-ray diffraction and differential thermal analyses of natural and synthetic tridymite led to the suggestion that tridymite may not be a pure silica polymorph. Hill and Roy (1958), however, successfully synthesized tridymite from transistor-grade silicon and high-purity silica gel using only H_2O as a flux, thus confirming the legitimacy of tridymite as a stable silica polymorph.

Tridymite in its region of stability between 867 and 1470°C is hexagonal with space group $P6_3/mmc$. The structural data for ideal high-temperature tridymite is based upon a fundamental stacking module in which sheets of silica tetrahedra are arranged in hexagonal rings (Table 1.7

Table 1.6 Structural data for quartz.

| | β -Quartz | | α -Quartz | |
|-----------------------------|-----------------------|----------|------------------|----------|
| Unit cell | | | | |
| a (Å) | 4.997 7 | | 4.912 39(4) | |
| c (Å) | 5.460 1 | | 5.403 85(7) | |
| V (Å ³) | 118.11 | | 112.933 | |
| ρ (g/cm ³) | 2.533 4 | | 2.649 5 | |
| Space group | $P6_422$ | $P6_222$ | $P3_121$ | $P3_221$ |
| | <i>Atom positions</i> | | | |
| $x(\text{Si})$ | 1/2 | 1/2 | 0.470 1 | 0.529 9 |
| $y(\text{Si})$ | 0 | 0 | 0 | 0 |
| $z(\text{Si})$ | 0 | 0 | 1/3 | 2/3 |
| $x(\text{O}_i)$ | 0.207 2 | 0.207 2 | 0.413 9 | 0.586 1 |
| $y(\text{O})$ | 0.414 4 | 0.414 4 | 0.267 4 | 0.732 6 |
| $z(\text{O})$ | 1/2 | 1/2 | 0.214 4 | 0.785 6 |

Data for β -quartz at 590°C from Wright and Lehmann (1981) and α -quartz at 25°C from Will et al. (1988).

Table 1.7 Structural data for high-temperature tridymite.

| Space group | $P6_3/mmc$ | | |
|-----------------------------|------------|-----|-----------|
| Unit cell | | | |
| a (Å) | 5.052(9) | | |
| c (Å) | 8.27(2) | | |
| V (Å ³) | 182.8(3) | | |
| ρ (g/cm ³) | 2.183 | | |
| Atom | x | y | z |
| Si(1) | 1/3 | 2/3 | 0.0620(4) |
| O(1) | 1/3 | 2/3 | 1/4 |
| O(2) | 1/2 | 0 | 0 |

Data for 460 °C from Kihara (1978).

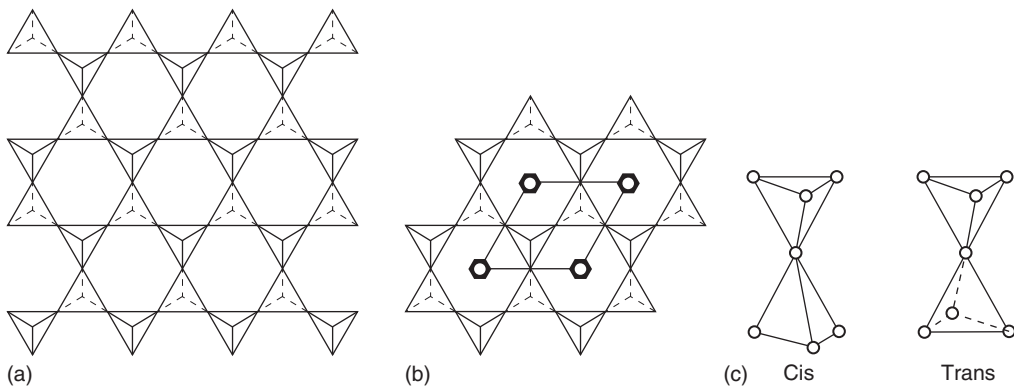


Figure 1.2 (a) Diagram of the tetrahedral sheet that serves as the fundamental stacking module in tridymite and cristobalite. In tridymite, the layers are stacked in a double AB sequence parallel to c , and in cristobalite, the sheets create a tripred ABC repeat along [111]. (b) Projection of the structure of ideal high-temperature tridymite along c . Adjacent tetrahedral layers are related by mirror symmetry, and the six-membered rings superimpose exactly. (c) The cis and trans orientations of paired tetrahedra. High-temperature tridymite tetrahedra adopt the less stable cis orientation, which maximizes repulsion among basal oxygen ions. In β -cristobalite, the tetrahedra occur in the trans orientation. Source: After Heany (1994).

and Figure 1.2). When standard tridymite is cooled below 380 °C, several phase inversions occur with various changes in symmetry. These tend to produce a large shrinkage and therefore a high thermal coefficient of expansion between 0 and 200 °C, almost $40.0 \times 10^{-6}/\text{K}$.

Cristobalite. The stable form of silica above 1470 °C is cristobalite. This phase is easily formed metastably in many glass-ceramic materials and can be cooled to room temperature in the same way as tridymite and quartz. Structurally, cristobalite is also formed from the fundamental stacking module of sheets of silica with hexagonal rings, but the orientation of paired tetrahedra are in the trans orientation as opposed to the cis orientation of tridymite (Figure 1.2). This leads to a cubic instead of a hexagonal morphology. In fact, the ideal β -cristobalite is a cubic analog of diamond such that silicon occupies the same positions as carbon, and oxygen lies midway

Table 1.8 Structural data for cristobalite.

| Space group | β -Cristobalite | α -Cristobalite |
|-----------------------------|-----------------------|-------------------------------------|
| | <i>Fd3m</i> | <i>P4₁2₁2</i> |
| Unit cell | | |
| <i>a</i> (Å) | 7.126 37 | 4.969 37 |
| <i>c</i> (Å) | — | 6.925 63 |
| <i>V</i> (Å ³) | 361.914 | 171.026 |
| ρ (g/cm ³) | 2.205 | 2.333 |
| Atom positions | | |
| <i>x</i> (Si) | 0 | 0.300 6 |
| <i>y</i> (Si) | 0 | 0.300 6 |
| <i>z</i> (Si) | 0 | 0 |
| <i>x</i> (O) | 1/8 | 0.239 2 |
| <i>y</i> (O) | 1/8 | 0.104 9 |
| <i>z</i> (O) | 1/8 | 0.178 9 |

Data for ideal β -cristobalite at 300 °C and α -cristobalite at 30 °C from Schmahel et al. (1992).

between any two silicon atoms. The space group for this structure is *Fd3m*, and the structural data for both cubic β -cristobalite and the low-temperature tetragonal alpha form are shown in Table 1.8.

The phase-transition temperature between low and high modifications of cristobalite does not appear to be constant, but a typical temperature is around 215 °C. The transition is accompanied by large changes in thermal expansion. The *a*- and *c*-axis of α -cristobalite increase rapidly at the rates of 9.3×10^{-5} and 3.5×10^{-4} Å/K, respectively; whereas in β -cristobalite, *a* expands at only 2.1×10^{-5} Å/K. This behavior translates into very large, spontaneous strains of –1% along *a*-axis and –2.2% along *c*-axis during inversion.

Stuffed Derivatives of Silica Buerger (1954) first recognized that certain aluminosilicate crystals composed of three-dimensional networks of (SiO₄) and (AlO₄) tetrahedra are similar in structure to one or another of the silicon crystalline forms. These aluminosilicates were termed “stuffed derivatives” because they may be considered silica structures with network replacement of Si⁴⁺ by Al³⁺ accompanied by a filling of interstitial vacancies by larger cations to preserve electrical neutrality. As would be expected, considerable solid solution generally occurs between these derivatives and pure silica. The stable silica polymorphs cristobalite, tridymite, and quartz all have associated derivatives, as does the metastable phase keatite. Examples include the polymorphs carnegieite and nepheline (NaAlSiO₄), which are derivatives of cristobalite and tridymite, respectively; β -spodumene (LiAlSi₂O₆), a stuffed derivative of keatite; and β -eucryptite (LiAlSiO₄) a stuffed derivative of β -quartz.

There has been both confusion and misunderstanding concerning the nomenclature of stuffed derivatives of silica in both the lithium and magnesium aluminosilicate systems. Roy (1959) was the first to recognize a complete solid-solution series between β -eucryptite (LiAlSiO₄) and silica with the structure of β -quartz. Most of the series higher than Li₂O:Al₂O₃:3SiO₂ in silica was found metastable except very near pure silica. Roy coined the term silica O to describe this β -quartz solid solution. This term has been discredited largely

because these phases are not of pure silica composition and, in fact, may be as low as 50 mol% silica as in the case of β -eucryptite. Moreover, the pure silica endmember is β -quartz itself.

The term virgilite was more recently proposed (French et al. 1978) for naturally occurring representatives of lithium-stuffed β -quartz solid solutions falling between the spodumene stoichiometry $\text{LiAlSi}_2\text{O}_6$ and silica. Virgilite was further defined as including only those compositions with more than 50 mol% $\text{LiAlSi}_2\text{O}_6$. The problem with this definition is that it arbitrarily reserves a specific part of the solid-solution range for no apparent reason. Moreover, the term virgilite was coined long after these materials had been widely referred to as β -quartz solid solution in the ceramic literature.

The term silica K was similarly initially coined by Roy (1959) to describe another series of solid solutions along the join SiO_2 – LiAlO_2 , which are stable over a wide range of temperatures. The compositions range from below 1 : 1 : 4 to about 1 : 1 : 10 in $\text{Li}_2\text{O}:\text{Al}_2\text{O}_3:\text{SiO}_2$ proportions (Figure 1.3) (Levin et al. 1964). Although it was initially recognized that this tetragonal series had a similar structure to the metastable form of SiO_2 , namely, keatite, originally synthesized by Keat (1954) at the General Electric Company, phase equilibria studies showed a large miscibility gap between pure SiO_2 keatite and the most siliceous endmember of this series (Figure 1.3). Since the term β -spodumene $\text{LiAlSi}_2\text{O}_6$ (1 : 1 : 4) was widely in use, it seemed reasonable to refer to this more limited solid-solution series as β -spodumene s.s. The term stuffed keatite has also been used to describe this solid solution, but since there is no continuous composition series to silica, the mineral name β -spodumene, which identifies the general composition area, is preferred. This is consistent with standard usage as in the case of nepheline or carnegieite

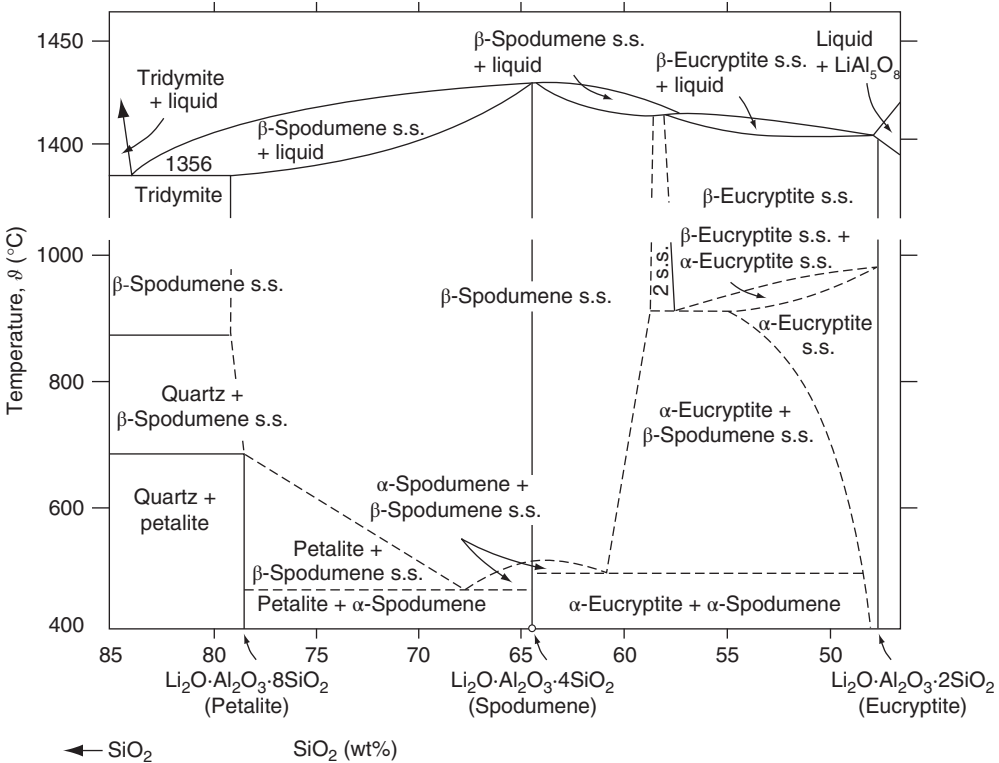


Figure 1.3 The phase diagram of the SiO_2 - $\text{Li}_2\text{O}-\text{Al}_2\text{O}_3$ - 2SiO_2 system. Source: After Levin et al. (1964) and Strnad (1986).